

Synthesis, Characterization and Study of Thermal Properties of New Silicone Polymers and Their Nanocomposites

Thikra A. Naif  , Basma J. Ahmed*  

Department of Chemistry, College of Education for Pure Science Ibn Al-Haitham, University of Baghdad, Baghdad, Iraq
*Corresponding Author

Received 28/01/2024, Revised 26/05/2024, Accepted 28/05/2024, Published Online First 20/10/2024



© 2022 The Author(s). Published by College of Science for Women, University of Baghdad.

This is an open access article distributed under the terms of the [Creative Commons Attribution 4.0 International License](https://creativecommons.org/licenses/by/4.0/), which permits unrestricted use, distribution, and reproduction in any medium, provided the original work is properly cited.

Abstract

This study aims to synthesize a new class of silicon polymers P_1 - P_4 were synthesized based on dichlorodimethylsilane (DCDMS) with some organic compounds containing terminal hydroxyl groups were synthesized for the first time [M_1 - M_4] via condensation polymerization. Also, their nanocomposites P'_1 - P'_4 were prepared in the presence of 0.7% the silver nanoparticles (Ag-NPs) using the solution casting method. The structures of all monomers and polymers were characterized by FTIR and 1H -NMR spectroscopy, which allowed to identify functional groups of monomers and silicone polymers. Thermogravimetric analysis (TGA) and differential scanning calorimetry (DSC) test were performed to analyze thermal behavior and effect of the presence of silver nanoparticles. The results of thermal analysis showed that the presence of phenyl rings demonstrated the thermal stability of pure silicon polymers, and the introduction of silver nanoparticles of 7% weight showed an improvement in the thermal performance of nanocomposites P'_1 - P'_4 compared to pure silicon polymers. Which means that the temperature for weight loss (TGA) was higher for the most nanocomposite P'_1 - P'_4 , where the TGA for polymers increased from 127 for polymer P_2 to 196 for its nanocomposite P'_2 , this may be due to filling the free voids between the Polymerized chains by silver nanoparticles. The silver nanoparticles were characterized and analyzed using X-ray diffraction XRD and scanning electron microscopy. The X-ray study showed the presence of silver nanoparticles and the average size of nanoparticles ranged from 20 -30 nanometers. The surface study was performed using scanning electron microscopy which showed a fairly uniform shape for the silver nanocomposites.

Keywords: Dichlorodimethylsilane, Nanocomposite, Silicone polymer, Silver nanoparticles, Thermal analysis.

Introduction

In recent years, many chemical and physical modifications have been made to polymers for the purpose of generating new hybrid polymers, an example of this type of polymers are those based on mixing silicon with hydrocarbon compounds to combine organic and inorganic properties¹. In the field of preparing hybrid polymers, thermal stability and good mechanical and chemical properties can be achieved, and they can also be used to improve optical properties², fluorescence³, ionic

conductivity⁴, and electrical and biochemical activity. There are also a lot of important devices that rely on hybrid materials. Sensors and electrochemical devices such as actuators, batteries, and supported capacitors, as well as photovoltaic electrochemical energy conversion cells, are an example of this type of technology^{5,6} significant chemical activity can be achieved using hybrid materials. Silicone resin is low molecular weight compounds with a high glass transition temperature.

They are materials with broad application. They have outstanding heat resistance, water resistance, and ultraviolet resistance and increase the stickiness of the surface of the adhesive⁷. It is possible to control the molecular weight and diversify the water resistance ability of the silicone resin and the thermal stability according to the composition and the functional group added. The addition of phenyl groups within the structure of silicone polymers increases the thermal stability and hydrophobic character, adding to a significant improvement in the overall properties of the polymers, offering new possibilities for their use and development as a new class of materials^{8, 9}. Polymers containing C=N bonds are considered an alternative to conjugated polymers, they are usually thermally stable and environmentally resistant polymers, are also antibacterial, antifungal, or cytotoxic activities but

Materials and Methods

All the raw materials were supplied from Merck and SIGMA-ALDRICH CO, as for silver nanoparticles (Ag-NPs) were obtained from Areege Alfurat company <https://vymaps.com/IQ/-105980260831569/>. X-ray diffraction via (Shimadzu-XR-6000) device with Nickel -Copper filter for the X-ray radiation (Cu K α , $\lambda = 1.5406 \text{ \AA}$). Scanning has continuously achieved under ($2\theta = 5-80$) range and in average speed of 5 degree / min. Atomic force microscopy (AFM) analysis were carried out on a microscope model SPM AA3000 Angstrom Advanced Inc., USA origin, thermogravimetric analysis (TGA) and differential scanning calorimetry were taken for by using (DSC-60A) origin Germany with an average heat rate of 5 degrees Celsius per minute, measurements of the scanning electron microscopy (SEM) via MIRA3 device. Atomic force microscopy

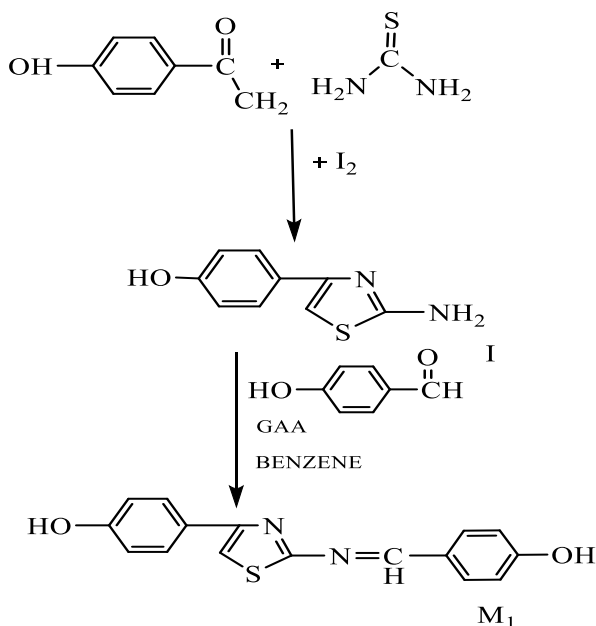
Synthesis monomers M₁ and M₂

The compounds 4-(2-aminothiazol-4-yl) phenol (I) and 4-(4-aminophenyl) thiazol-2-amine (II) were preparing according to the literature^{12, 13} Iodine 3.8 g, 0.015 mol, thiourea 2.28 g, 0.03 mol were mixed with 4-hydroxy acetophenone 2.04 g, 0.015 mol or 4-amino acetophenone 2.025 g, 0.015 mol and on the water bath it was heated for melting for 8 hours, then cooled, washed with diethyl ether, filtrated the solid then washed with solution of sodiumthiosulfate, the precipitated was filtered and re-crystallized from ethanol, then the monomers M₁ and M₂ were synthesized by using 0.001 mol, 0.002 mol

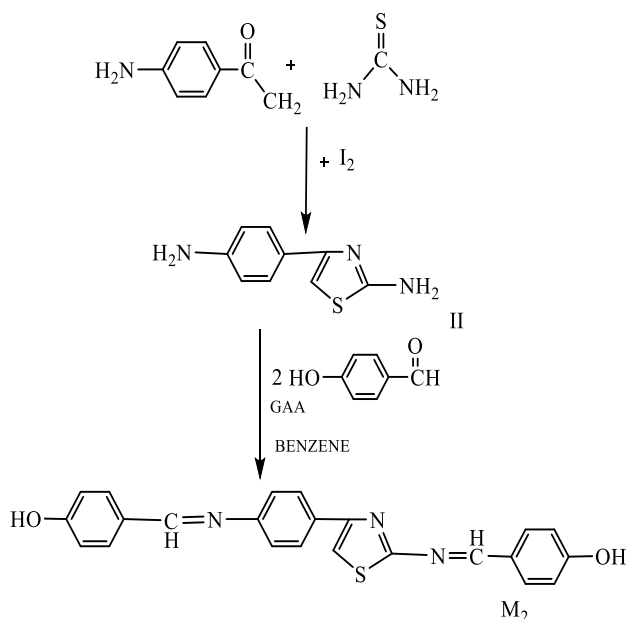
the low solubility and high melting or softening temperatures are the main drawbacks of polyaromatic polymers containing C=N bonds. Thus to improved processability of high molecular weight polymers, could be achieved by introduce silicon moieties within the rigid conjugated aromatic azomethine structures^{10, 11}.

The purpose of this work was to synthesize new monomers that have aromatic structure to improve the thermal stability of silicone polymers and study the effect presence of silver nanoparticles on the thermal stability. The thermal stability was investigated by DSC and TGA. X-ray diffraction analysis (XRD), scanning electron microscopy (SEM) and atomic force microscopy (AFM) were used to demonstrate the confirmed the presence of the silver nanoparticles (Ag-NPs) and surface morphology, respectively.

respectively from aldehyde and 3 drops of glacial acetic acid (GAA) in dry benzene 5mL the reaction mixture refluxed for 10 hrs¹⁴, then applying vacuum. Under vacuum the solvent come off and the precipitate recrystallize from ethyl acetate. The physical data and structure of the synthesized compounds M₁ and M₂ are listed in Tables 1, Schemes 1 and 2. shows the reactions to form compounds I, II, M₁ and M₂. The FTIR spectrum of compounds I and II showed the disappearance absorption bands at 1660 cm⁻¹ due to C=O stretching of 4-hydroxy acetophenone with appearance of stretching bands in the region 3427- 3184 due to asymmetry and symmetry NH₂ groups, the FTIR spectrum of monomers M₁ and M₂ showed the disappearance absorption band of NH₂ group of starting materials (I and II) with appearance of stretching bands in the region 1647- 1640 due to azomethine C=N groups.



Scheme 1. Reaction pathways to synthesis compound M₁

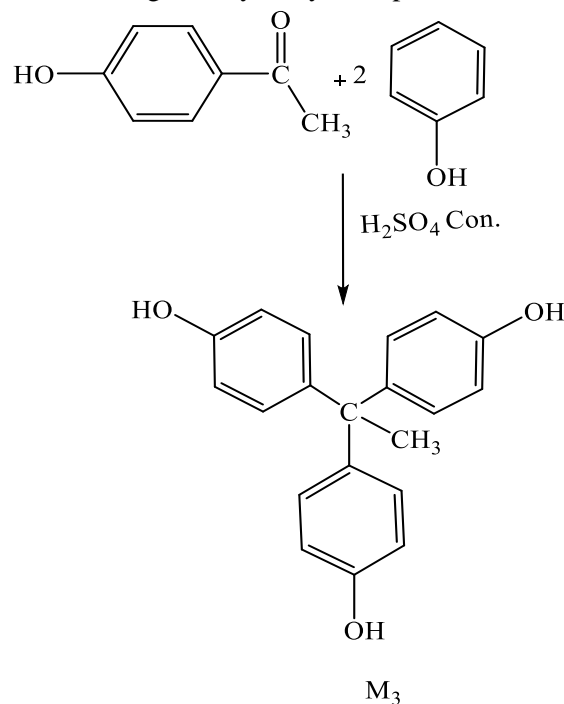


Scheme 2. Reaction pathways to synthesis compound M₂

Synthesis monomer M₃

A mixture of phenol 2.72g, 0.02mol with 4-acetophenone 1.22g, 0.01mol and H₂SO₄ as a catalyst 2.5 mL was heated in the oil bath at 60°C for 7 hrs. then cooled and reaction mixture was transferred to cold water 10 mL^{15,16}. The precipitate collected by filtration, washed by cold water and re-crystallized from ethanol, the physical data, structure of the synthesized monomer M₃ are listed in Table 1 and

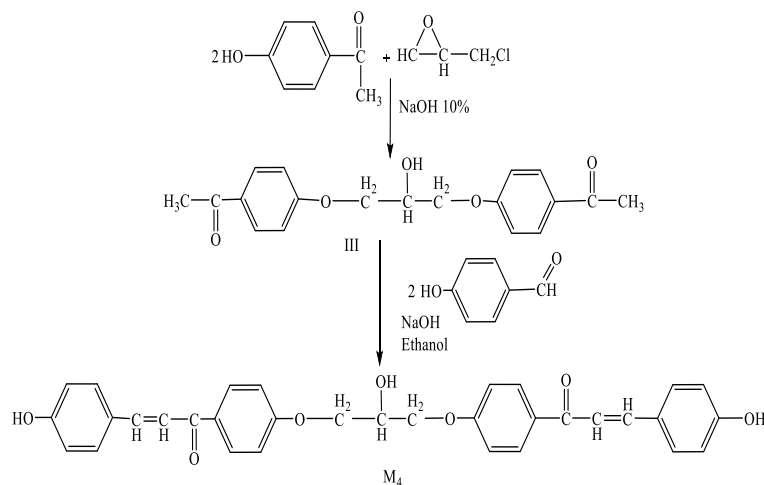
Scheme 3. outlined the reaction to form monomer M₃. The FTIR spectrum of compound M₃ showed the disappearance absorption bands at 1660 cm⁻¹ due to C=O stretching of 4-hydroxyacetophenone.



Scheme 3. Pathway for synthesis M₃

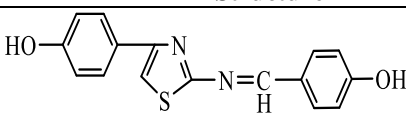
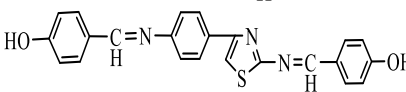
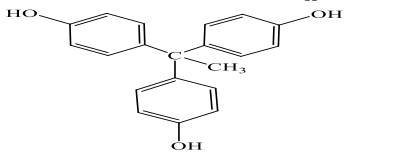
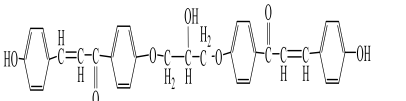
Synthesis monomer M₄

A quantity of 4-hydroxyacetophenone 2.72 g, 0.02 mol was dissolved in 10% aqueous NaOH in oil bath at 60°C. The mixture was refluxed with stirring for 1 hrs followed by addition of epichlorohydrin 0.92g, 0.01mol. Then the temperature was raised to over 90°C and the reaction continued for another 2 hrs. until precipitate separated out, the precipitate was filtered, washing for many times with distil water and neutralized with 5 mL solution cold from dilute HCl (5%)¹⁷, then the product (III) was dried after that, the a mixture of the compound(III) 3.28g,0.01mol and 4-hydroxybenzalehyde 2.44g, 0.02mol were dissolved in 5mL of ethanol. NaOH solution 0.02 mol was added slowly with stirred for 3hrs and after the reaction mixture has been cooled, put in 200 mL the ice water with stirrer and kept in refrigerator for 24 hrs¹⁸.The precipitate M₄ obtained was filtered, washed and recrystallized from ethyl acetate. The physical data and structure of the synthesized monomer M₄ are listed in Table 1, and Scheme 4. outlined the reaction to form monomer M₄. The FTIR spectrum of monomer M₄ showed the appearance of stretching bands at 1640 cm⁻¹ due to C=C alkene group.



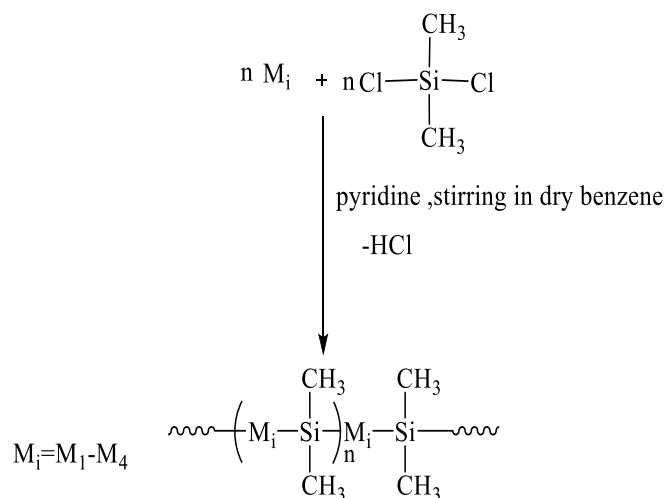
Scheme 4. Pathway for synthesis M₄

Table 1. Summary of physical properties for monomers

NO. Monomer	Structure	Color	M.P.
M ₁		yellow	134-137
M ₂		yellow	154-158
M ₃		orange	244-250
M ₄		off white	128-130

Synthesis polymers (P₁-P₄)

These silicon polymers were synthesized by the condensation reaction 0.1 mol of one of the monomers (M₁-M₄) in dry benzene with 0.1 mol dimethyldichlorosilane in the presence of 0.5mL pyridine with stirring under a temperature of 0-4 in an ice water bath for 12 hrs. The resulted solid was poured onto 10 mL solution cold from dilute HCl (5 %) then the precipitate was filtered, dried and recrystallized from diethyl ether¹⁹. Scheme 5. illustrates general formula for synthesized silicone polymers P₁-P₄. The physical data of the synthesized polymers (P₁-P₄) are listed in Table 2.



Scheme 5. Structure of silicon polymers (P₁-P₄) with different monomers

Table 2. Summary of physical properties for polymers

NO. polymer	Color	Softing point
P ₁	Light brown	142
P ₂	pistchio	127
P ₃	Dark red	101
P ₄	Brown	140

Synthesis silver nanocomposites (P₁-P₄)

Results and Discussion

FTIR and ¹HNMR characterization

All silicone polymers showed a broad peak near 910-952 cm⁻¹ belonging to Si-O-ph bond, which indicates the formation of Si-O-ph main chain in the silicone polymer. The characteristic peak near 1400-1433 cm⁻¹ indicated the presence of Si-CH₃, and the peak around 2910-2980 cm⁻¹ belonged to the C-H bond of Si-CH₃ groups. While, the absorption peak around 3000-3043 cm⁻¹, which belonged to the C-H bond of the benzene ring in silicone polymers, in addition a stretching band for C=N group to the polymers P₁ and P₂ appeared between 1612-1652 cm⁻¹. The characteristic FT-IR absorption bands for monomers M₁-M₄ and polymers P₁-P₄ were listed in the Table 3.^{12,22} The ¹HNMR spectrum for all monomers and polymers was in DMSO as a solvent. The ¹HNMR spectrum for monomers M₁ showed the following signals: signal at δ 10.627 ppm could be attributed for one proton of OH and proton of CH=N group at δ 9.788 ppm, signals in region δ (7.952-7.027) ppm for protons of benzene rings and one proton of thiazol ring appear at δ 6.950, and M₂ showed the following signals: signal at δ 10.619 ppm and signal at δ 9.788 ppm. could be attributed for one proton of OH and proton of CH=N group, respectively, signals in region δ (7.888-7.044) ppm for protons of benzene rings and one proton of thiazol ring appear at 6.946 ppm, The ¹HNMR spectrum for monomer M₃ exhibited: signals in δ 9.108 ppm and region δ (7.224-6.620) ppm that attributed for proton of OH phenol ring and protons of benzene rings, respectively and protons of CH₃-C group appeared signal at δ 1.242 ppm. The ¹HNMR spectrum for monomer M₄ showed the following signals: signal in δ 10.700 ppm for proton of OH, multiple signals between δ (7.938-7.134) ppm and single at δ 6.965 ppm that attributed for protons of benzene rings and protons of CH=CH

Polymers nanocomposites were produced by using the solvent casting method 1g of the one of the polymers (P₁-P₄) has been put in 5 ml of dimethylmethanamide (DMF) with stirring using magnetic stirrer for 6 hrs. Then silver nanoparticles were added with a weight of 7% to solution polymer under magnetic stirring after that, used ultrasonic water bath for 6 hours at 35°C to ensure dispersion nanoparticles within silicone polymer, the mixture was poured into petri dishes then put in an oven for 2 hrs. to get rid of the remaining solvent²⁰⁻²³.

group, respectively other signals at δ 3.777 ppm and δ 3.656 ppm could be attributed for one proton of CH-OH and protons of CH₂-O groups, respectively. The ¹HNMR spectrum for polymer P₂ showed the following signals: signal in δ 9.725 ppm and δ 9.695 ppm could be attributed for one proton of OH in end of chain and proton of CH=N group, respectively, signals in region δ (8.826-6.819) ppm for protons of benzene rings and one proton of thiazol ring, another signal at δ 0.1 ppm is attributed for protons of ((CH₃)₂-Si) groups. The ¹HNMR spectrum for polymer P₃ exhibited: signals in δ 9.023 ppm and region δ (8.870-6.545) ppm that attributed for proton of OH phenol ring and protons of benzene rings, respectively and protons of CH₃-C group appeared signal at δ 1.986 ppm, signals in region δ (0.013-0.994) ppm for protons of ((CH₃)₂-Si) groups. The ¹HNMR spectrum for polymer P₄ showed the following signals: : signal in δ 9.927 ppm for proton of OH, multiple signals between δ (9.872-6.997) ppm and single at δ 6.976 ppm that attributed for protons of benzene rings and protons of CH=CH group, respectively another signals at δ 3.454 ppm and δ 2.559 ppm could be attributed for one proton of CH-OH and protons of CH₂-O groups, respectively, while the protons of ((CH₃)₂-Si) groups appeared in region δ (0.047-0.0.135) ppm.^{7,22,24} Whereas ¹³C NMR spectrum for P₂, (in DMSO as a solvent) showed: signal at δ 191.39 ppm due to C=N (C2) carbon atom of thiazole ring²⁵ and at δ 164.09 ppm for C=N carbon atom of azomethine. Two signals at δ 143.93 ppm and δ 133.17 ppm assigned to C=C (C4) carbon atom and C=C (C5) carbon of thiazole ring, four signals at δ (129.13-127.09) ppm are due to aromatic carbon atoms for benzene ring, also four signals are in the region δ (116.60-115.97) ppm for C=C carbon atoms of another benzene ring, ¹³C NMR spectrum for P₄

showed: signal at δ 196.292 ppm belong to the carbon of the carbonyl group C=O t, signal at δ 162.07 ppm Due to the OCH₂ carbon (next to the phenyl ring), two signals at δ 120.89 ppm and δ 142.94 ppm belong to the alpha-carbon and the beta-

carbon, respectively for C=C group. There are five signals in the δ (116.03 -114.05) ppm for the C=C carbon atoms in the benzene rings, while the signal at 10.88 ppm can be assigned to Si-CH₃.

Table 3. Summary of FTIR spectra of the monomers and polymers.

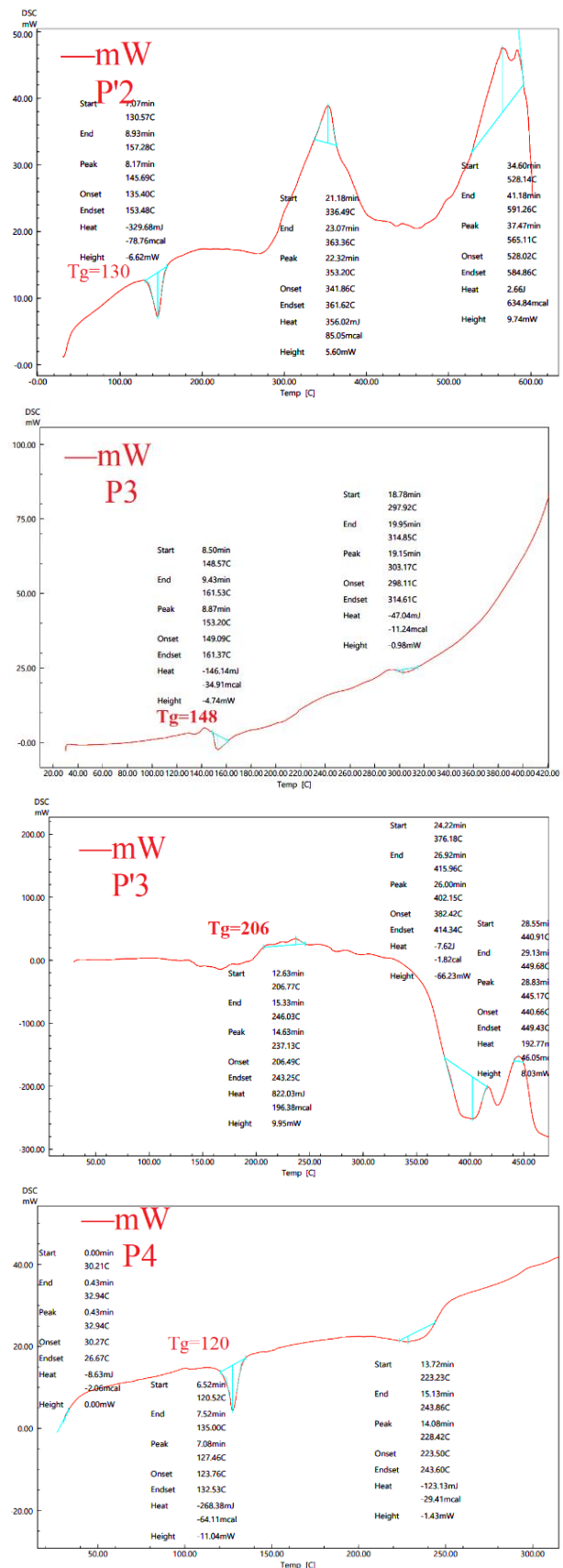
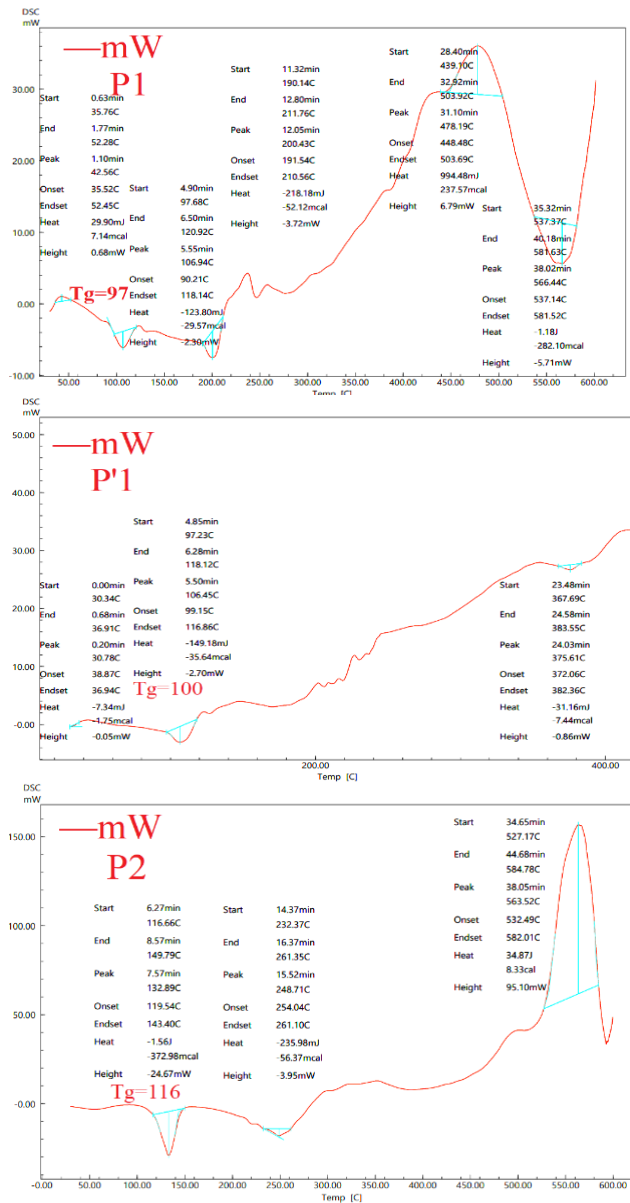
Compound index	cm ⁻¹							
	OH	C-H aromatic	C-H aliphatic	C=N end, exocyclic	C=C	Si-CH3 asymmetric, symmetric	Si-OPh	others
I	3240	3010	—	1627	overlap	—	—	NH ₂ 3427, 3190 C-S-C 695 C-S-C 640
M ₁	3190	3010	—	1647	1597	—	—	C-S-C 644
P ₁	3213	3024	2962-2742	1612	1593	1400,1230	910	C-S-C 644
II	—	3000	—	1625	1579	—	—	NH ₂ 3304,3184 C-S-C 659 C-S-C 643
M ₂	3192	3043	—	1640	1597	—	—	C-S-C 643
P ₂	3211	3028	2966-2754	1652	1595	1421,1240	952	640
M ₃	3417	3000	2980-2800	—	1589	—	—	—
P ₃	3406	3024	2958-2802	—	1604	1433,1251	933	—
III	3367	3000	2931,2742	—	1600	—	—	C=O keton 1681
M ₄	3236	3000	2910-2870	—	1597	—	—	C=O keto. 1670 C=Calkene 1640
P ₄	3203	3026	2968-2831	—	1598	1415,1240	946	C=O Ket. 1670 C=C alkene 1640

DSC and TG analysis

DSC is analytical technique that measures the heat flow rate (mW=mJ/sec) to or from a sample as it is subjected to controlled temperature program. DSC scan for the silicone polymers and their nanocomposites gave the same thermal degradation trend for most polymers and their nanocomposites. The physical glass transitions appeared in the ranges of 97- 148°C and 100- 206°C for silicon polymers and their nanocomposites, respectively as shown in Table 4, Fig. 1 show the DCS graph for silicone polymer P₁-P₄ and nanocomposites P'₁-P'₄. It was noted from the diagram that silicon polymers with more phenylene units showed higher thermal stability compared to what is known to the dimethylsilicone polymer²². In general, silicon polymers with AgNPs content are more stable compared to those without AgNPs. In the Fig. 1, P₂ showed of multiple endothermic peaks in the DSC heating curves. The glass phase transition temperature (T_g) was at about 116.66°C, Enthalpy (H-1.56J), followed by melting

processes at about 248.71°C (H-235.98mJ). While the its nanocomposite P'₂ showed T_g at 130.57 °C followed by peak at about 145.69 °C (H-329.68mJ) refer endothermic peak and 353.20°C(H356.02mJ) refer to crystallization temperature. This result suggests a good dispersion of AgNPs, dispersed nanoparticles are able to promote the cold crystallization²⁶. Most of the TGA thermograms of polymers and their silver nanocomposites are shown two stages of weight loss. The TGA curve began to drop slightly around 71 -196°C probably due to evaporation of moisture content, while the main decrease of TGA curve started in range 200-250 °C due to the beginning of the disintegration. The main regression of TGA curve started from 142 for P₁, 136 for P'₁, 127 for P₂, 196 for P'₂, 101 for P₃, 127 for P'₃ and 140 for P₄, 149 for P'₄. this means that the temperature of weight loss in most nanocomposite structures was higher compared to pure silicon polymers, which could be due to filling the free spaces between the polymeric chains with silver

nanoparticles^{22,27,28}. Fig. 2 shows the TGA graph for silicone polymer P₁-P₄ and nanocomposites P'₁-P'₄, respectively. In Fig. 2, the thermogravimetric analysis showed significant weight loss for polymers P₃ and P₄ at 550°C, while other samples P₁ and P₂ have significant residue left at the same temperature that may be related to the presence of the thiazole ring which give amore thermal stability to the polymer P₁ and P₂. The results of thermogravimetric analysis (TGA) are listed in Table 5.



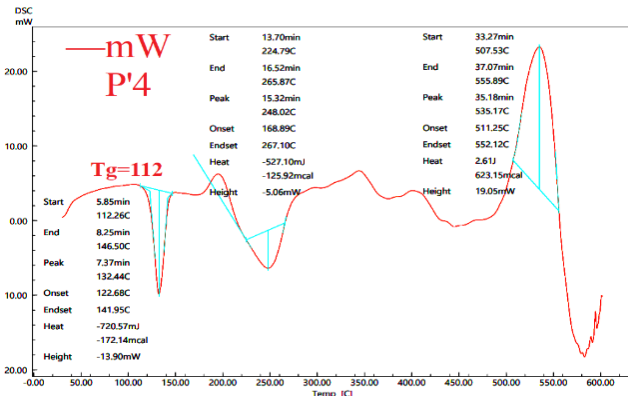
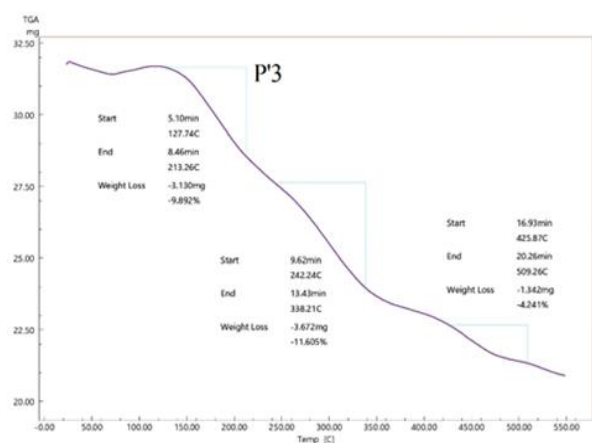
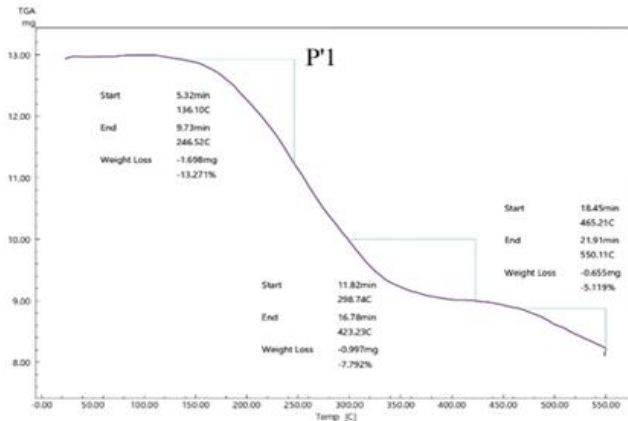
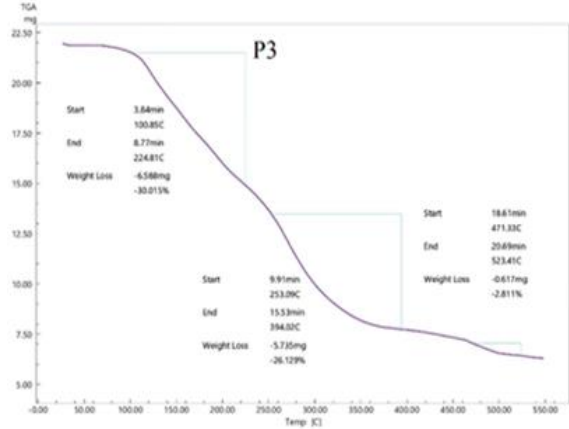
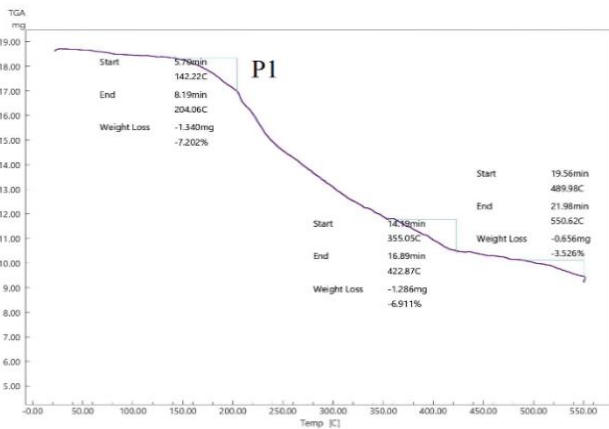
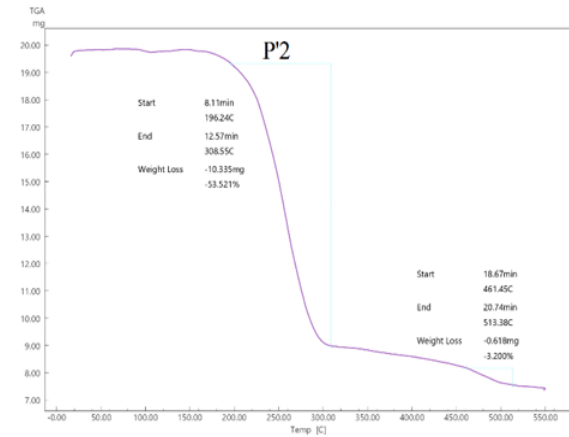
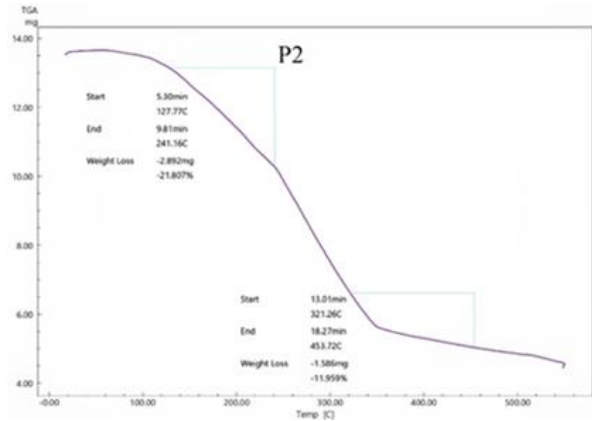


Figure 1. DSC curves of silicone polymers P₁-P₄ and silver-nanocomposites P'₁-P'₄, -containing 7% AgNPs

Table 4. Glass transition temperature of silicon polymers and their nanocomposites

Pure silicone polymer	Glass transition temperature (T _g) (°C)	Nano composite	Glass transition temperature (T _g) (°C)
P ₁	97	P' ₁	100
P ₂	116	P' ₂	130
P ₃	148	P' ₃	206
P ₄	120	P' ₄	112



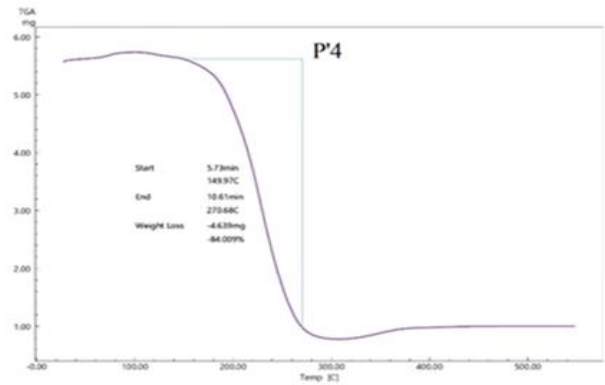
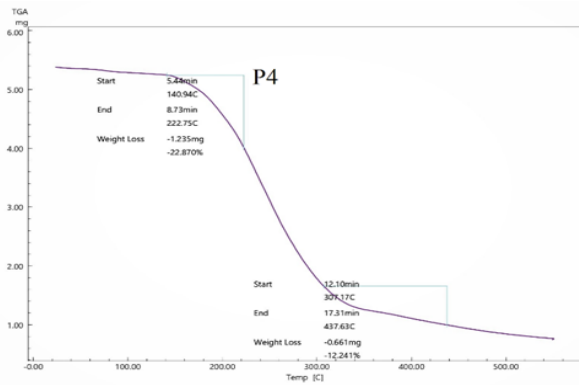


Figure 2. TGA curves of silicone polymers (P₁-P₄) and silver-nanocomposites (P'₁-P'₄)-containing 7% AgNP

Table 5. Thermogravimetric analysis of silicon polymers and their nanocomposites

Sample no.	Temperature for Degradation Onset temperature (°C)	Temperature for 50% mass loss (°C)	Temperature for maximum Degradation (°C)	Residue at 550°C (%)
P ₁	142	290	550	82%
P' ₁	136	270	550	73%
P ₂	127	255	459	66%
P' ₂	196	255	513	43%
P ₃	101	225	523	41%
P' ₃	127	290	509	81%
P ₄	140	250	437	65%
P' ₄	149	225	270	16%

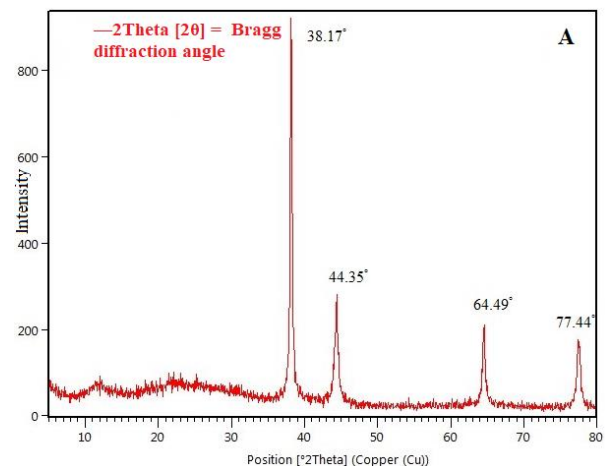
XRD analysis

By X-ray diffraction (XRD) the crystal structures of silver nanoparticles (AgNPs), polymer and nanocomposite were investigated as shown in Fig. 3 XRD has proven that pure AgNPs alone have four peaks at $2\theta = 38.17^\circ$, and another at 44.35° , 64.49° , and 77.44° , and these peaks comply to the reflections of crystal standards 111, 200, 220 and 311 in the face-centered cubic structure (FCC) of silver metal based on the database on JCPDS with file no.04-0783²⁹, by Debye-Scherrer formula, the average size of AgNPs can be determined.

$$D = \frac{K\lambda}{\beta \cos \theta}$$

K (Scherrer constant) = 0.89, λ (X-ray wavelength) = 0.15406, β stands for the peak width at half-maximum height (FWHM) and θ stands for Bragg diffraction angle, The average size of AgNPs has been recorded between 20 to 30 n. The polymer peaks P₁ appeared at 15.85° , 31.92° and 24.23° , while

the silver nanocomposite exhibited the six main peaks comply to the four peaks in the AgNPs and three peaks to polymer with a decrease in an intensity of these peaks, this is expected to occur due to the creation of non-crystalline regions resulting from the intercalation of a polymer with silver particles.²¹



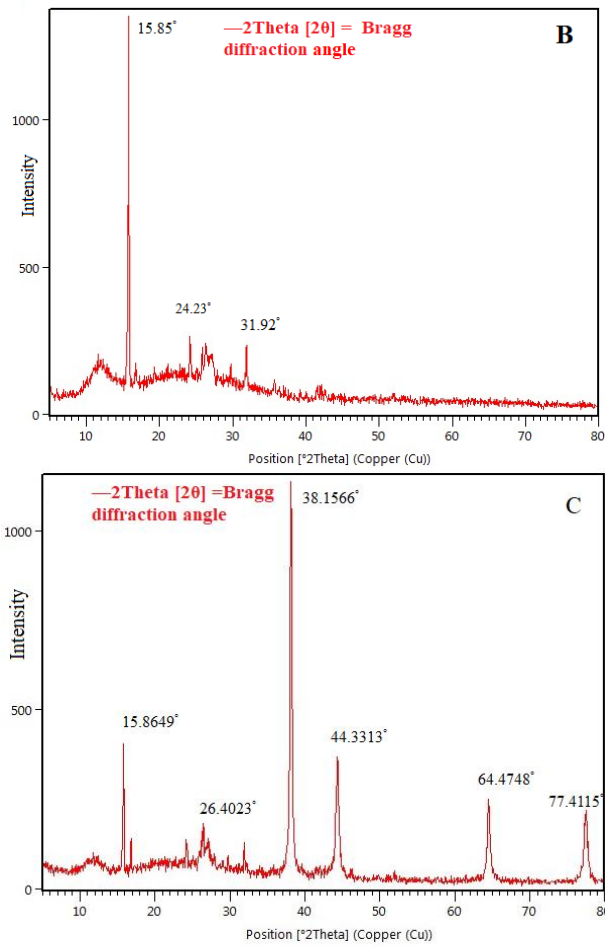


Figure 3. X-ray diffraction patterns with Copper filter for the x-ray radiation of (A) silver nanoparticles, (B) polymer P₁ and (C) silver nanocomposite P'₁.

Atomic force microscopy

The surface morphology of silver nanoparticles and polymer with nanocomposites was investigated using atomic force microscopy AFM. Fig. 4 shows the AFM images for AgNPs, while polymer P₁, and the distribution of the nanoparticles (AgNPs) in nanocomposite P'₁ are shown in Fig. 5. The morphological characteristics were closely related to the crystallinity. It can be seen from the Fig. 4 that the nanoparticles have spherical morphology with an average size of 20-30 nm, this is consistent with the XRD results. Comparing the AFM images between nanocomposite and pure polymer, it is noted that the polymer image showed a fairly homogeneous surface with the absence of Ag particles as shown in Fig. 5 a and b. The image c and d showed a nanoparticles dispersed almost uniformly within the matrix with some agglomerates appearing.

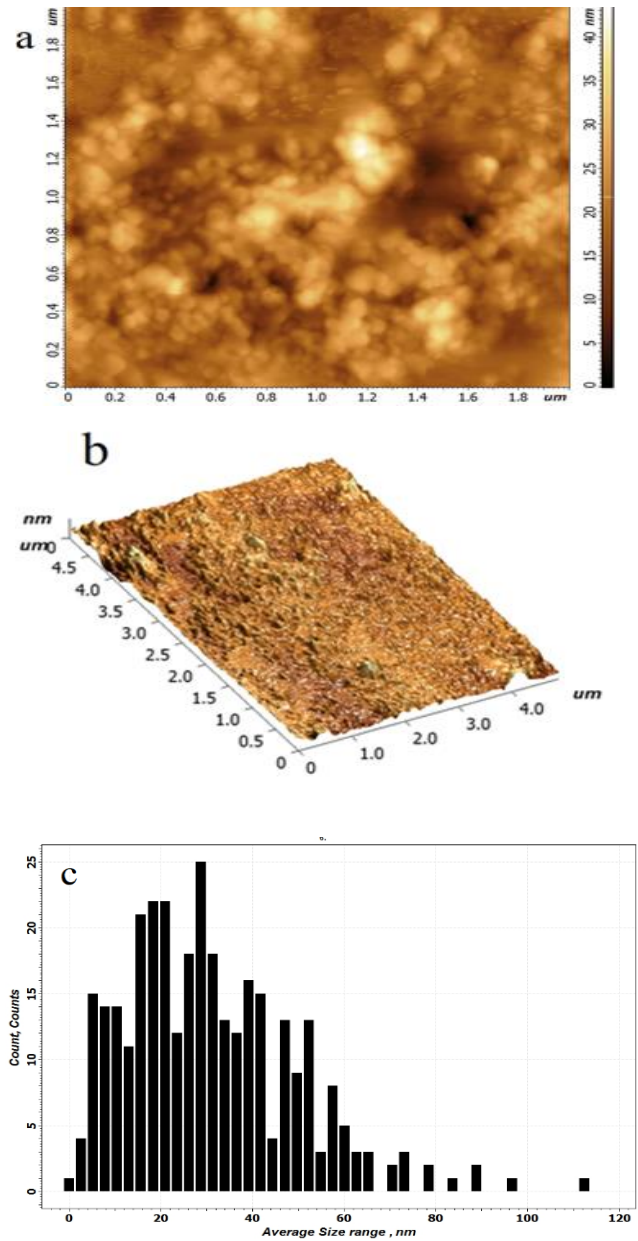
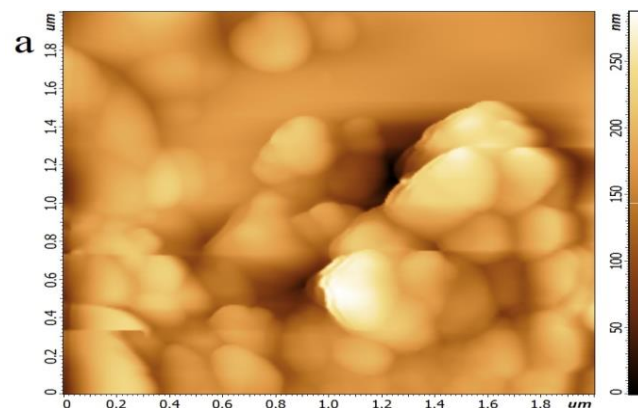


Figure 4. AFM images (a) and (b) of the silver nanoparticles, (c) histogram of granularity accumulation distribution for AgNPs



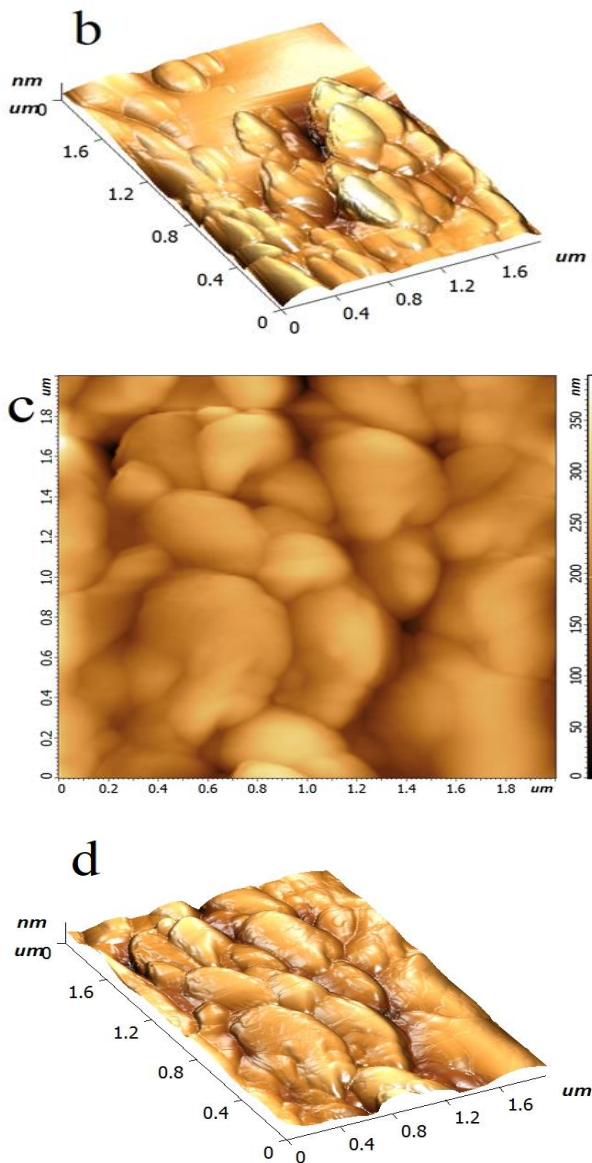
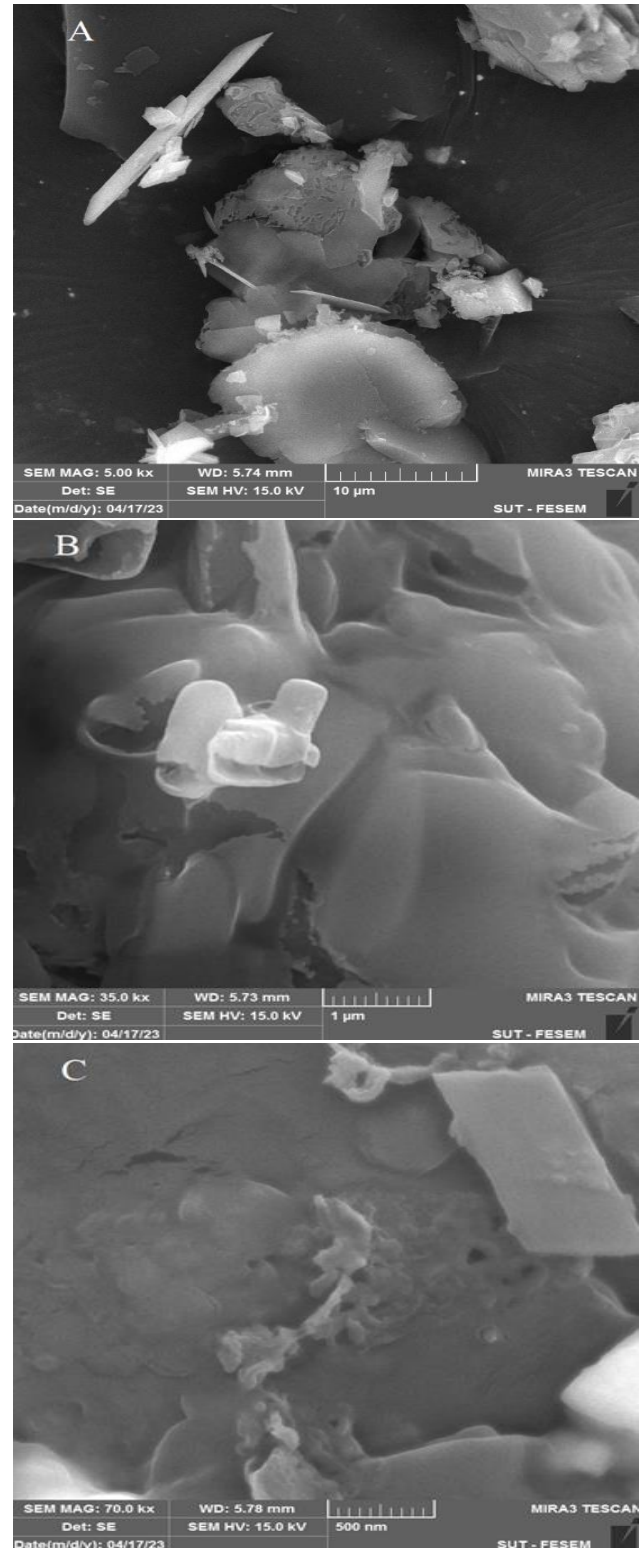


Figure 5. Atomic force microscope (AFM) images of a, b for polymer P₁ and c, d for silver nanocomposite with 7% AgNPs.

Morphology study

The silicone polymer P₁ has miscibility with the silver nanoparticles and leads to various morphologies. Fig. 6 shows SEM images for the P₁ and P₁. The nanocomposite P₁ showed surface contains some narrow breaking paths. The comparison between pure polymer and hybrid system P₁ showed that hybrid had the fracture paths are branched and less continuous than in the case of

the pure polymer and showed P₁ slightly rough surface, and also discontinuous, twisted.



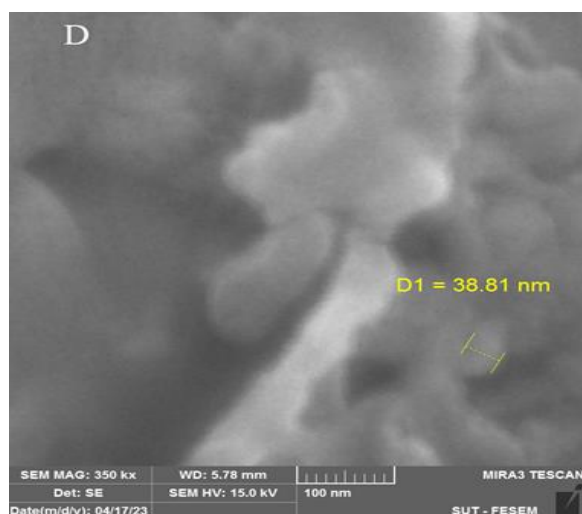


Figure 6. SEM images of surfaces A, B for P₁ and C,D for P'₁

Conclusion

In this study, Silicon polymers were synthesized by condensation polymerization using dichloro(dimethyl) silane (DCDMS) with various organic compounds, subsequently, their nanocomposites were also synthesized in the presence of silver nanoparticles (AG-NPS) using the solution casting method. The structure of these polymers was indicated by using FTIR and ¹HNMR. The effects of p-phenylene units on the thermal stability of silicone polymers were investigated by DSC and TGA, which demonstrated enhanced thermal stability with increasing phenylene units. On the other hand, the effect of the silver nanoparticles (AgNPs) contents on thermal properties for silicone polymer composites was investigated. The thermal stability of the composites show improvement with the presence of 7 % AgNPs, as shown by the DSC

testing result. DSC testing of the composites revealed the higher glass transition temperature (T_g) in presence of AgNPs, which are 100 for P'₁, 130 for P'₂, 206 for P'₃ and 112 °C for P'₄ compared to the T_g values for pure silicone polymers 97, 116, 148, and 120 °C for P₁, P₂, P₃ and P₄, respectively. Which means that the temperature for weight loss (TGA) was higher for the most nanocomposite P'₁-P'₄. The crystal structure of silver nanoparticles alone through XRD analysis showed four peaks, and the presence of AgNPs in the prepared nanocomposite was also detected. AFM analysis revealed that the Ag particles had a spherical morphology with an average size of 20-30 nm with some accumulation and SEM analysis revealed that the nanoparticles were almost uniformly distributed within the matrix as well as numerous agglomerates could also be seen.

Acknowledgment

The authors would like to thank the staff of the Service Laboratory, College of Science, University

of Baghdad and University of Basra for their support of this research.

Authors' Declaration

- Conflicts of Interest: None.
- We hereby confirm that all the Figures and Tables in the manuscript are ours. Besides, the Figures and Images, which are not ours, have been given permission for re-publication attached with the manuscript.
- No animal studies are present in the manuscript.

- No human studies are present in the manuscript.
- No potentially identified images or data are present in the manuscript.
- Ethical Clearance: The project was approved by the local ethical committee at University of Baghdad

Authors' Contribution Statement

All authors contributed to the study conception and design. T.A.N., did the sample preparation and

analysis and B.J.A. was responsible for the writing original draft, review and editing last version.

References

1. Coyalaltzin PG, Aurelio RH, Gustavo RP, Alejandro AS, Andres AC, Gerardo GG. et al. Synthesis and Characterization of the Starch/silicone Oil Composite and Elaboration of its Films. *Silicon*. 2022; 14(8): 4157-4167. <https://doi.org/10.1007/s12633-021-01209-x>
2. Guodong Su, Aili W, Mingming Zh, Hengbo Y, Guoxi Wang. Selective Synthesis of Triethoxysilane and Tetraethoxysilane through Direct Reaction between Ethanol and Silicon Catalyzed by CuCl and Metallic Cu⁰ Nanoparticles in Fixed-bed Reactor. *Silicon*. 2022; 14(2): 573-580. <https://doi.org/10.1007/s12633-020-00830-6>
3. Navarut P, Kasimanat V, Makoto O. Heterostructural transformation of mesoporous silica-titania hybrids. *Sci Rep*. 2021; 11(3210): 1-12. <https://doi.org/10.1038/s41598-020-80584-8>
4. Chayma O, Manel E, Giuseppe B, Sonia A, Antonio S, Zouhaier A. Structural, vibrational, optical properties and theoretical studies of new noncentrosymmetric material: Bis (2-Amino-5-(methylthio)-1,3,4-thiadiazol-3-ium) Pentachloroantimonate. *J Mol Struct*. 2021; 1240(130538): 1-14. <https://doi.org/10.1016/j.molstruc.2021.130538>
5. Hiroki I, Shuta H, Shigeru S. Skillful Control of Dispersion and 3D Network Structures: Advances in Functional Organic-Inorganic Nano-Hybrid Materials Prepared Using the Sol-Gel Method. *Polymers*. 2022; 14(16): 3247. <https://doi.org/10.3390/polym14163247>
6. Arunkumar L, Vaibhav M, Manjunath KP, Sangappa KG. Synthesis, characterization and studies of BaFe₂O₄/PMMA nanocomposite. *Polym Bull*. 2021; 78(4): 5905-5921. <https://doi.org/10.1007/s00289-020-03403-0>
7. Rui H, Jinshui Y, Qihong M, Dan P, Hui Z, Zhizhou Y. Study on the Synthesis and Thermal Stability of Silicone Resin Containing Trifluorovinyl Ether Groups. *Polymers*. 2020; 12(10): 2284. <https://doi.org/10.3390/polym12102284>
8. Chenwei S, Dan W, Caihong X, Wenyi Ch, Zongbo Z. Comparative study on polysilazane and silicone resins as high-temperature-resistant coatings. *High Perform Polym*. 2022; 34(4): 474-486. <https://doi.org/10.1177/09540083211069041>
9. Elizaveta S, Mati D, Valdek M, Sergei B. Comparative study of perhydropolysilazane protective films. *Surf Eng*. 2022; 38(7): 769-777. <https://doi.org/10.1080/02670844.2022.2155445>
10. Ying Z, Ralf G, Wei L, Farhan J, Ralf R. Evaluation of mechanical properties and hydrophobicity of room-temperature, moisture-curable polysilazane coatings. *J Appl Polym. Sci*. 2021; 138(21): 50469. <https://doi.org/10.1002/app.50469>
11. Amira AM, Abeer AN, Sadeek AS, Hazem SE. Synthesis and Spectral, Thermal and Antimicrobial Investigation of Mixed LigandMetal Complexes of N-Salicylidene Anilineand 1,10-Phenanthroline. *Compounds*. 2023; 3(1): 298-309. <https://doi.org/10.3390/compounds3010022>
12. Nisreen H Karam, Jumbad H Tomma, Ammar HD, Nasreen R Jber. Synthesis And Liquid Crystalline Behaviour of New Series Containing 1, 3-Oxazepine And 1, 3-Thiazole Rings. *ANJS*. 2014; 17(4): 67-75. *JIARM*
13. Nisreen HK, Alaa K Sh, Ammar HD. Synthesis, characterization and study of mesomorphic behavior of new bent and linear core compounds containing heterocyclic rings, *Mol Cryst Liq Cryst*. 2021; 731(1): 66-79. <https://doi.org/10.1080/15421406.2021.1966871>
14. Ahmed BJ, Maida HS, Fadhel SM. Synthesis and Study of the Antimicrobial Activity of Modified Polyvinyl Alcohol Films Incorporated with Silver Nanoparticles. *Baghdad Sci J*. 2023; 20(5): 1643-1653. <https://dx.doi.org/10.21123/bsj.2023.7471>
15. Khalil T, Alireza K, Ali D, Milad Kh. Efficient Ru^{III}-catalyzed synthesis of 9-aryl-9H-xanthene-3,6-diols as precursors to fluorones. *Chin Chem Lett*. 2012; 23(2): 165-168. <https://doi.org/10.1016/j.ccllet.2011.11.012>
16. Anupam GB, Lata PK, Piyooosh A Sh, Asha BT, Rabindra K N, Sushant K Sh. et al. A facile microwave assisted one pot synthesis of novel xanthene derivatives as potential anti-inflammatory and analgesic agents. *Arab J Chem*. 2016; 9(1): S480-S489. <https://doi.org/10.1016/j.arabjch.2011.06.001>
17. Ridzuan M, Mohammad B O, Hanafi I, Zulkifli A. Synthesis and characterization of rigid aromatic-based epoxy resin. *M P J*. 2009; 4 (2): 68-75.
18. Nebras MJ, Dhuha FH, Jumbad HT. Synthesis and Characterization New Schiff Bases, Pyrazole and Pyrazoline Compounds Derived From Acid Hydrazide Containing Isoxazoline Ring. *Ibn al-Haitham J Pure Appl Sci*. 2014; 27 (3): 435-447.
19. Mengqiu J, Chaobo W, Wei L, Dahai G. Synthesis and characterization of a silicone resin with silphenylene units in Si-O-Si backbones. *J Appl Polym Sci*. 2009; 114(2): 971-977. <https://doi.org/10.1002/app.30635>
20. Hileuskaya KS. et al. Hydrothermal Synthesis and Properties of Chitosan-Silver Nanocomposites. *Russ J Inorg Chem*. 2021; 66(8): 1128-1134. <https://doi.org/10.1134/S0036023621080064>

21. Maida HS, Ahmed BJ. Synthesis, characterization and Study Bioactivity of Silver Nanocomposites. Int J Pharm Res. 2020; 12 (4): 766-772. <https://doi.org/10.31838/ijpr/2020.12.04.134>
22. Zhizhou Y, Shuang H, Rong Z, Shengyu F, Changqiao Z, Shengyou Z. Effects of silphenylene units on the thermal stability of silicone resins. Polym Degrad Stab. 2011; 96(12): 2145-2151. <https://doi.org/10.1016/j.polymdegradstab.2011.09.014>
23. Balqees M Al, Hanaa J K. Nano composites of PAM Reinforced with Al₂O₃. Baghdad Sci J.2022; 20(6): 2300-2306. <https://doi.org/10.21123/bsj.2023.7353>
24. Jumbad H T, Omar B O, Ammar H D.A new thiazolidinone and triazole derivatives: Synthesis, characterization and liquid crystalline properties, J Mol Struct. 2022; 1270(5): 133817. <https://doi.org/10.1016/j.molstruc.2022.133817>.
25. Wasan M. H, Jumbad H. T, Rajaa K. Synthesis and Study the Biological Activity of New Heterocyclic Compounds Derived From Hydrazide Derivatives. Indian J Forensic Med Toxicol. 2020; 14 (4): 1881-1887. <https://doi.org/10.37506/ijfmt.v14i4.11819>
26. Ilaria C, Elena F, Debora P, Jose M K, Francesca N. Effect of silver nanoparticles and cellulose nanocrystals onelectrospun poly(lactic) acid mats: Morphology, thermal propertiesand mechanical behavior. Carbohydr Polym. 2014; 103(1): 22– 31. <https://doi.org/10.1016/j.carbpol.2013.11.052>
27. Vikneswari S, Mohamed Th H, Radzi AM, Ahmad AS, Ain U M, Syafiqah N A. et al. Effect of Silver Nanopowder on Mechanical, Thermal and Antimicrobial Properties of Kenaf/HDPE Composites. Polymers. 2021; 13(22): 3928. <https://doi.org/10.3390/polym13223928>.
28. Shaker Q, Hadee M N, Suhad M A, Hemn U A, Husam A, Jawad A. et al. Fly Ash-Based Geopolymer Composites: A Review of the Compressive Strength and Microstructure Analysis. Mater. (Basel). 2022; 15(20): 7098. <https://doi.org/10.3390/ma15207098>
29. Muhammad F A , Mohd M M , Zaidah Z A , Irwan S , Muhammad S M, Muhammad A A. Synthesis, Characterisation and Antibacterial Properties of Silicone–Silver Thin Film for the Potential of Medical Device Applications , Polymers. 2021; 13 (21): 3822. <https://doi.org/10.3390/polym13213822>.

تحضير وتشخيص ودراسة الخواص الحرارية لبوليمرات السليكون الجديدة ومتراباتها النانوية

ذكري علي نايف، بسمه جعفر احمد

قسم الكيمياء، كلية التربية للعلوم الصرفة ابن الهيثم، جامعة بغداد، بغداد، العراق.

الخلاصة

الهدف من الدراسة تحضير فئه جديده من بوليمرات السليكون P₁-P₄ والتي تمت على اساس استخدام ثنائي مثيل ثنائي كلورو سيلان(DCDMS) مع بعض المركبات العضويه التي تحتوي مجاميع الهيدروكسيل الطرفيه والتي حضرت لأول مره M₄-M₁ ، بأستخدام البلمره التكتيفيه. كما تم تحضير متراباتها النانويه P'₁-P'₄ بوجود جسيمات الفضة النانويه (Ag-NPs) باستخدام طريقة صب المحاليل. شخصت جميع التراكيب للمونمرات والبوليمرات المحضره بأستخدام مطيافية FTIR و H¹NMR (لبعض البوليمرات) مما سمح بتحديد المجموعات الوظيفية الفعاله للمونومرات وبوليمرات السليكون. اجريت التحاليل الحراريه الوزنيه TGA والمسح المسعري التفاضلي DSC لتقييم السلوك الحراري وتأثير وجود جسيمات الفضة النانويه AgNPs. اظهرت نتائج التحليل الحراري ان وجود حلقات الفينيل اظهرت استقرار حراري لبوليمرات السليكون النقيه P₁-P₄ وان اقحام جسيمات الفضة النانويه بوزن 7 ٪ اظهرت تحسن في الاداء الحراري للمترابات النانويه P'₁-P'₄ مقارنة ببوليمرات السليكون النقيه، ممايعني ان درجة الحراره لفقدان الوزن TGA كانت اعلى لمعظم المترابات النانويه P'₁-P'₄ مقارنة الى بوليمرات السليكون النقيه، حيث ازادت درجة الحراره لفقدان الوزن TGA للبوليمر P₂ من 127 الى 196 للمترابه النانويه P'₂. وهذا قد يعود الى ملئ الفراغات الحره بين السلاسل البوليمريه بواسطة جسيمات الفضة النانويه. استخدمت تقنية حيود الأشعه السينيه XRD لتشخيص وجود جسيمات الفضة النانويه حيث اظهرت XRD وجود الفضة بحجم نانوي يتراوح بين 20-30 نانوميتر بالإضافة الى دراسة شكل وحجم جسيمات الفضة بتقنية مجهر القوة الذريه وكما تم دراسة مورفولوجية السطح باستخدام تقنية مجهر المسح الالكتروني والذي اظهرنوعا ما سطح موحد للمترابه النانويه.

الكلمات المفتاحية: ثنائي كلورو ثنائي مثيل سيلان ، المترابات النانويه ، بوليمرات السليكون، جسيمات الفضة النانويه، التحليل الحراري.